Fatigue Lifetime Events Detected Using Acoustic Emission Technique

Samuel Charca, Amilcar Quispitupa, Basir Shafiq*

School of Engineering, University of Puerto Rico, Mayagüez, PR 00681

ABSTRACT

Fatigue crack initiation and growth process of model AA7075-T6 subjected to simulated marine environment and varying stress ratio is studied using acoustic emission technique. The results indicate a significant reduction in crack initiation and overall lifetime when specimens were tested in the presence of marine environment, while an increase in fatigue life was observed as a function of increasing stress ratio. SEM fracture surface analysis exhibited intergranular, transgranular and cleavage as modes of failure. In general terms, Cleavage fracture produce lower AE signal amplitude, whereas, transgranular tearing produces an increment of signals amplitude. However, the correlation between those modes of failure with the AE results can be cumbersome since the AE signals are highly dependent upon the loading and environmental testing conditions.

Key Words: Acoustic Emission, Fatigue Life, SEM fracture modes, Corrosion Fatigue, AA7075-T6.

INTRODUCTION

The susceptibility of high strength aluminum alloys to failure in marine environment is principally attributed to the effect of hydrogen that enters into the material causing unpredictable failures /1/. Hydrogen evolution takes place as a result of partial reaction between the metal surface and the marine environment causing metal dissolution, hydrogen embrittlement and possibly formation of passive (oxide) film that is continuously ruptured to make crack growth possible /2-4/. The damage induced by hydrogen, however, is not easy to account for since the material remains apparently undamaged and cannot be detected by classical inspection methods /5,6/. The non-destructive AE technique has been found to be a useful alternative in many

* Corresponding Author: Phone: 787-832-4040 ext. 2094, Fax: 787-265-3816,
Email: basir_shafiq@uprm.edu

material systems that may help in conducting in-situ monitoring of aircraft components, such as, fuselage and arresting shanks, etc. suffering from environmental failures /7,8/. Failure (or internal damage) results from a rapid rupture of the material which signifies rapid release of energy that travels through the material in the form of transient elastic waves. Piezoelectric AE sensors mounted on the specimen surface are used to monitor and detect such stress waves. However, discerning AE signals can be a complex and challenging process as the output is a mixture of multitude of signals emanating from various cracking processes, background noise and friction, etc. /5,6,9/. Significant effort is generally required to classify and block the background noises. As it is difficult to eliminate the sources of all background noises during the testing, thresholds are set during the post processing of the data to filter out the undesired signals whenever possible. Use of AE requires substantial insight into the material behavior and AE signal processing. For example, the variations in the fatigue induced AE signals in high strength aluminum alloys are generally minute, erratic and the energy levels are too low for proper classification of failure events /6,9/. Therefore, the successful implementation of AE technique requires substantial preliminary calibration, parameters adjustment and threshold setups in order to filter out the undesirable signals and retain the meaningful AE data /9-11/. In-spite of these difficulties, precedence exists to suggest that with some effort, AE data can be classified and correlated to complex failure mechanisms, such as microcracking, creation and/or movement of dislocations, subcritical crack formation due to the effect of hydrogen and corrosion, etc., that may be otherwise missed /6/.

AE has been widely used to detect a variety of cracking processes; however, its use and success in fatigue of metals subjected to corrosive environment is somewhat limited /11,12/. This investigation makes an attempt to apply the AE technique to high strength alloys used in critical aircraft components in order to acquire an insight into the crack initiation and growth process and to understand the implementation and limitations of the AE technique. The specific tasks include studying the effect of marine environment and stress ratio on the fatigue lifetime of AA7075-T6 [strength ~537 MPa and toughness ~ 27MPa-$m^{1/2}$] that has been widely used in aircraft structural longeron and frame elements /13/. AE findings will also be verified by SEM analysis. This program is significant as a large inventory of aging Navy carrier based aircraft fleet while exposed to a multitude of corrosive agents operates under extremely high flight loads, thus the reliability becomes an important issue /13-15/.

EXPERIMENTAL SETUP

Tension-tension testing was performed on compact tension AA7075-T6 specimens in the presence of 3.5%NaCl and pH~2.5 (simulating marine environment) under load control at a frequency of 1 Hz and subjected to triangular waveform at a stress level of 15% of ultimate quasi-static load, while the stress ratio was varied between 0.1 and 0.7. Each sample was polished to a mirror finish in order to avoid any stress

concentration that could produce undesirable noise during the AE data collection. All the testing was performed at room temperature on servo-hydraulic fatigue testing machine equipped with traveling electron microscope. Crack length was measured using compliance technique in compact tension specimens that has been proven reliable in crack growth studies /16/, along with periodic visual inspections.

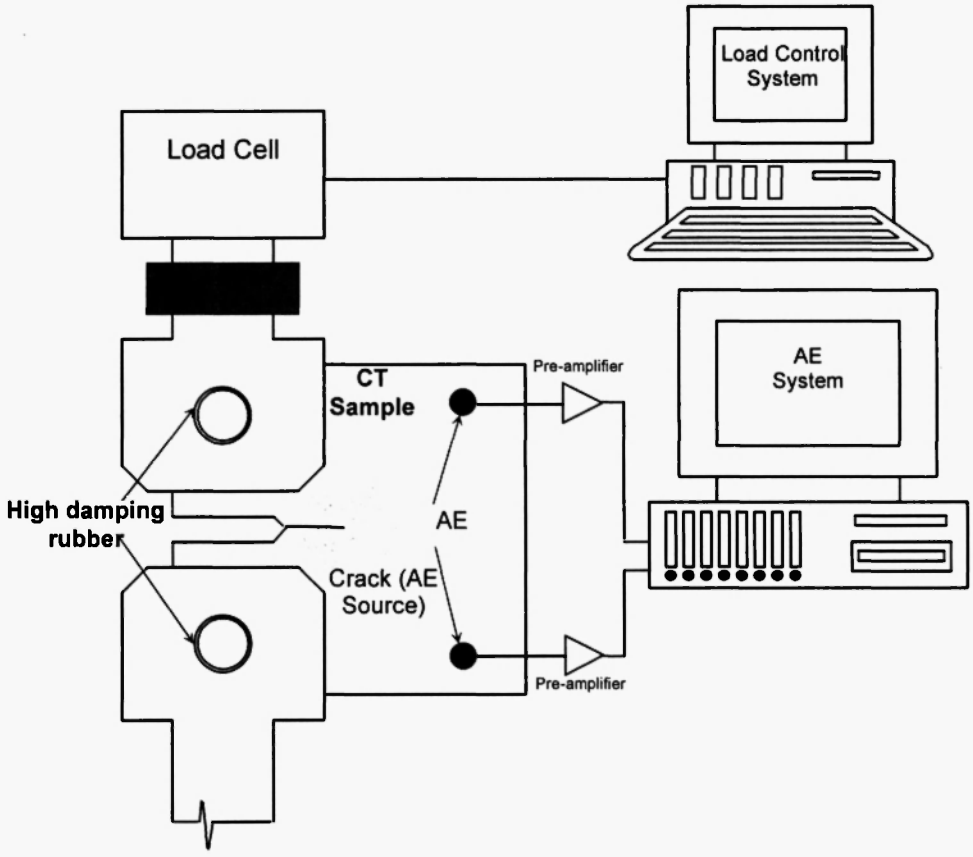

Fig. 1: Fatigue loading and AE monitoring setup in a CT sample test.

The AE signal parameters such as amplitude (dB), energy level (Volts^2 or MARSE as used in PAC systems /4/), duration (micro-sec) and cumulative counts were recorded and used to study the damage evolution and characterization in the AA7075-T6 specimens. The sketch of AE system with two Pico-sensors used in a linear array on the specimen surface at 30 mm distance from each other is shown in Fig. 1. ASTM E976 standard lead breaks of 0.5 mm diameter and 2H of hardness were used to calibrate the AE system and source location parameters /4/. AE signals can be classified as bursts, continuous and mixed. The AE signals of interest are bursts that contain useful information since they are generated by the formation of damage or crack increments in the specimen tested. While, continuous signals are generally produced by noise and rubbing. Thus, these unwanted signals must be discriminated. In order to minimize extraneous background

and frictional noise, high damping rubber was used around the loading pins while a threshold value of 35dB and filtering frequency of 10-1000 kHz were used. After significant preliminary testing and data processing, 20dB was found to be the most suitable pre-amplifier parameter, whereas, the AE software control system used 40dB of pre-amplifier /12/.

EXPERIMENTAL RESULTS

The presence of corrosive electrolyte increased the crack growth rates in specimens especially during stage II (stable crack growth regime) as compared to tests conducted in air at all stress ratios; however, the effect of electrolyte on the crack initiation time was less pronounced, as shown in Fig. 2. Crack initiation time was observed to reduce by an average of 52% while the overall lifetime was reduced by about 62% when the specimens were tested in the presence of corrosive marine environment at a stress ratio of 0.1, however, the effect was less severe at higher stress ratios, as can be seen in Figs. 2 and 3. Similar results have been reported in the literature /3,13/. Fig. 4 illustrates the AE results for AA7075-T6. For specimens evaluated in air, the AE activity had a decreasing trend as the stress ratio increased, whereas, for specimens tested in 3.5%NaCl solution an increasing trend was observed as a function of increasing the stress ratio, also indicated in Figs. 4.

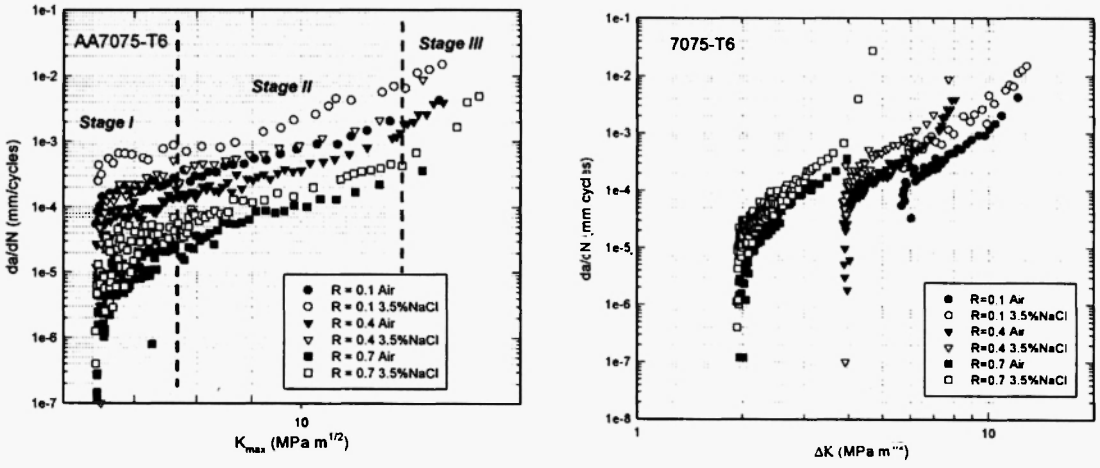

Fig. 2: da/dN vs. K_{max} curves divide in the characteristic, stage I, stage II and stage III .

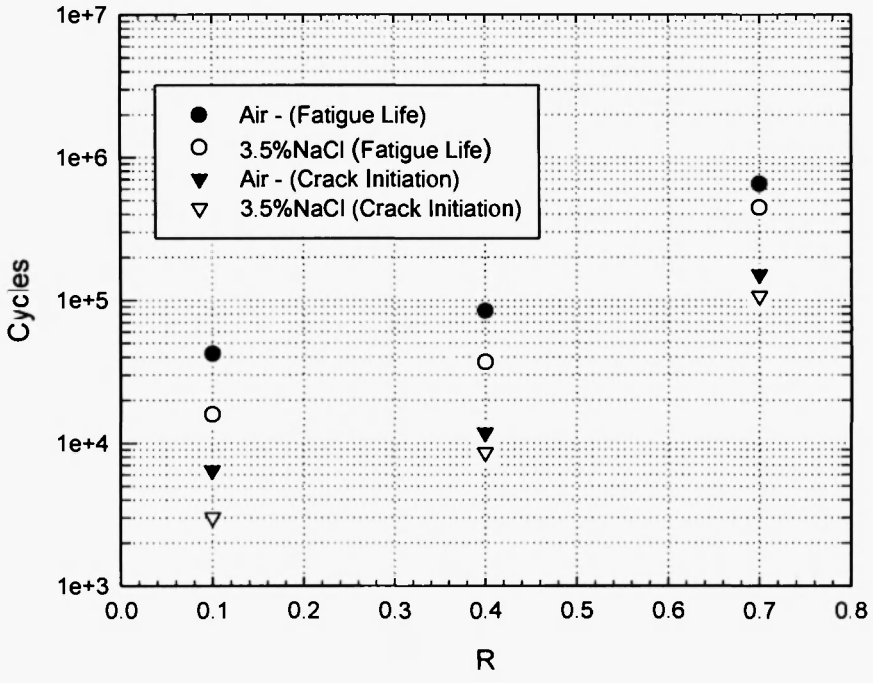

Fig. 3: Average crack initiation and failure at diverse R ratios for air and corrosion environment.

DISCUSSION

Various mechanisms simultaneously take place leading to the observed enhancement in the CGR. For example, coupled effect of stress and an increase in the potential difference due to the galvanic cell created between the crack tip and the rest of the material, facilitates ionic diffusion of aggressive anions like Cl^- down the crack length leading to dissolution of the bare metal surface due to localized metal loss (a metal dissolution process). Furthermore, dissolution of NaCl in H_2O causes the H^+ and OH^- ions to be "freed" more than otherwise and causes the dissociation of Na^+ and Cl^- ions such that overall conduction activity is increased. While Cl^- activity goes on in the metal dissolution process, H^+ simultaneously gets diffused as well in the material thereby weakening the material through reduction in bond strength. H^+ is much smaller than Cl^-, and therefore diffuses faster than Cl^-. The H^+ and OH^- produced subsequently react and/or get absorbed into the metal surface to form a brittle oxide film or a hydride phase or capture and move with the vacancies /17-19/. Brittle crack growth occurs as the film is ruptured and/or crack grows into brittle hydride phase by plastic strain. Combination of stress, and electrolytic medium such as aqueous NaCl increases chances of

hydrogen generation, increased mobility of Cl^-, weakening of atomic bonds (faster at the crack tip), and overall increase in the CFCG, as observed in Figs. 2 and 3. Migrating hydrogen atoms also occupy the microscopic faults and by combining with other hydrogen atoms produce a high local pressure that also contributes in the observed enhancement of crack initiation and growth process.

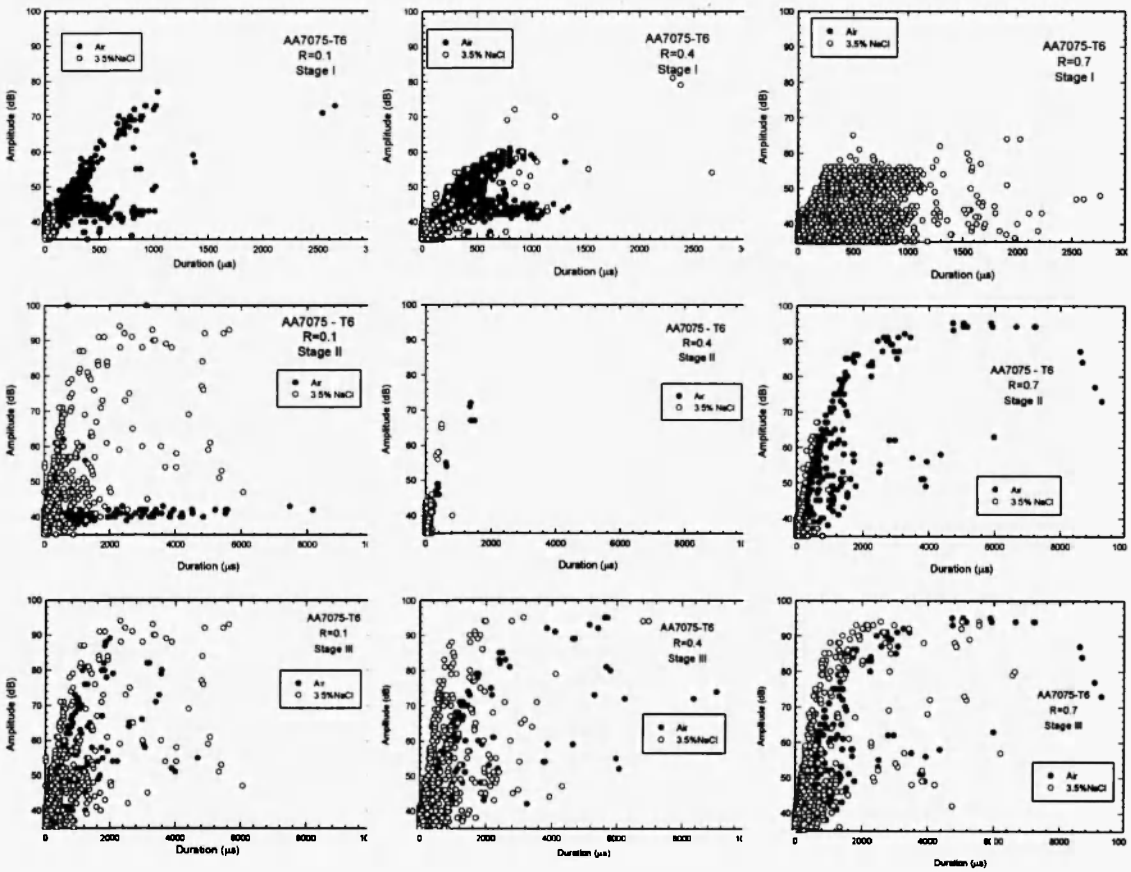

Fig. 4: Amplitude vs duration at various stress ratios and during different stages of crack growth.

As the observed CGR is higher at lower stress ratios, it implies an increased potential difference (or higher current density) as compared to specimens subjected to higher stress ratios. Increase in the current density leads to accelerated metal dissolution and production of hydrogen, while lower stress ratios promote preferential diffusion of hydrogen towards the crack tip (zone of high triaxial stress) /18/. Furthermore, the transport of corrosive species due to an enhanced cyclic pumping effect of corrosive solution is expected as the stress level is reduced, thus leading to an increase in the CGR.

The reduction in crack initiation and growth time can also be attributed to the load amplitude and its relationship to the microstructural changes. Aluminum alloys have been known to rearrange their

microstructure due mainly to enhanced dislocation mobility especially at the crack tip. Under fatigue loading, the effect of repeated microstructural rearrangement is expected to be a major contributing factor in the observed effect of stress ratio, as presented in Fig. 2. In addition, SEM analysis performed on AA7075-T6 samples corroborated the severity of the effect of stress ratio for specimens tested in air and in the presence of electrolyte. Fig. 5 exhibits significant changes in the fracture surface morphology under varying stress ratios during crack initiation and growth stages. At lower stress ratios, the fracture surface is characterized by the presence of transgranular tearing combined with cleavage fracture features caused by extrusion and intrusion for specimens tested in air, however, the transgranular tearing mode subsides as a function of increasing stress ratio and the cleavage-like fracture becomes dominant as exhibited in Fig. 5. These characteristics were observed under stage I and stage II of crack growth. The presence of electrolyte favored the intergranular fracture which was enhanced at high stress ratios. From Fig.3, the fatigue life of specimens evaluated under corrosion at R=0.7 was around 450 000 cycles which represent a significant time exposed to corrosion processes as opposed to almost an order of magnitude reduction in lifetime at R=0.1. Effect of corrosion is pronounced at regions of high heterogeneity (i.e. micro-faults, grain boundaries, inclusions, etc) that causes intergranular fracture as observed by SEM micrographs /20/. Intergranular crack paths tend to increase the CGR (because corrosion weakens the grain boundaries) compared to transgranular tearing mode (samples tested in air) as can be observed in SEM images of Fig. 5 /13/.

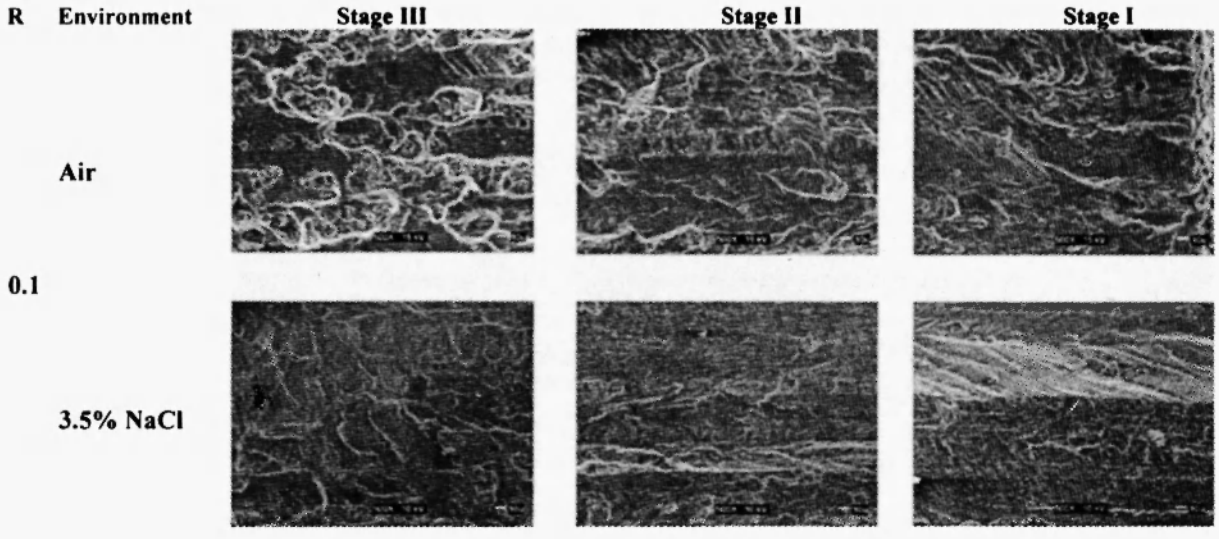

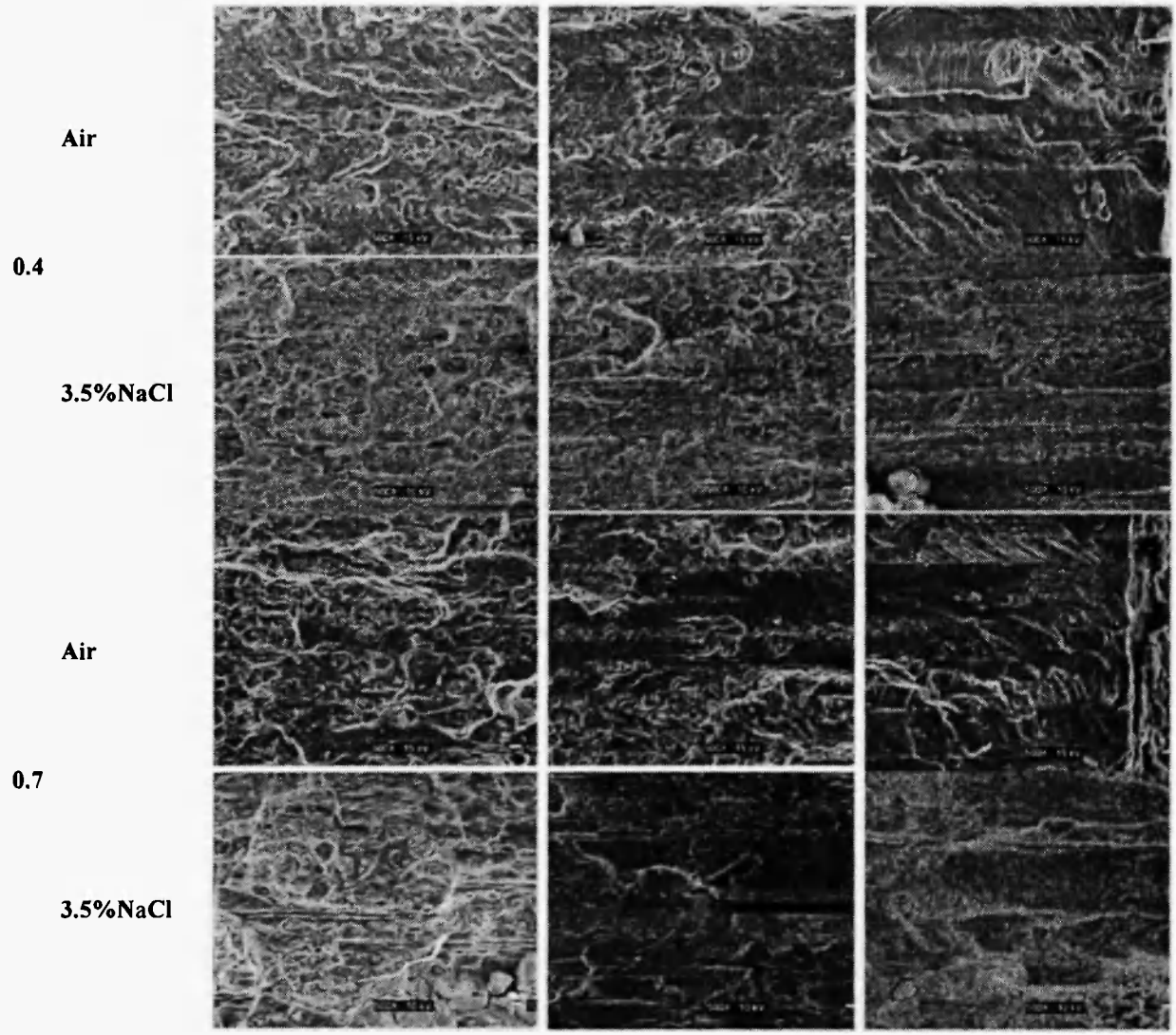

Fig. 5: SEM, fracture surface images in air and corrosion environment divided in three stages, right to left is the direction of crack growth.

During final stage III (onset of failure) the specimens exhibited a dominant microvoid and dimpled fracture appearance as can be seen in Fig. 5. The dimple phenomena can be attributed to microvoids formation and coalescence due to macroscopic plastic deformation which can be observed at high K values. Furthermore, it appears that the stress ratio and corrosive environment has no effect on the fracture appearance during this final stage.

To characterize the AE activity to detect failure, the classic approach consists of monitoring the hit counts and energy in a cumulative sense /4/. However, cumulative analysis carries high probability of error due to

the presence of external noises that can mask the actual events of the similar energy level. Each failure mode emits a distinct AE signal with a characteristic amplitude duration and frequency. As opposed to composite materials where AE technique has found a niche, metals have low damping ratio and as a result the amplitude and duration are not affected to the same extent as in composites /4,11,19/.

Classification of failure modes is generally performed by studying the amplitude, energy levels, hit counts and duration, etc., however, the problem becomes complex due to enormity of the data collected during a complete lifetime. After testing various approaches, data was grouped into the three stages of lifetime in the current study according to the classification outlined in Fig. 2, which facilitated data handling and comparative analysis of AE based failure characteristics, as shown in Figs. 4,6.

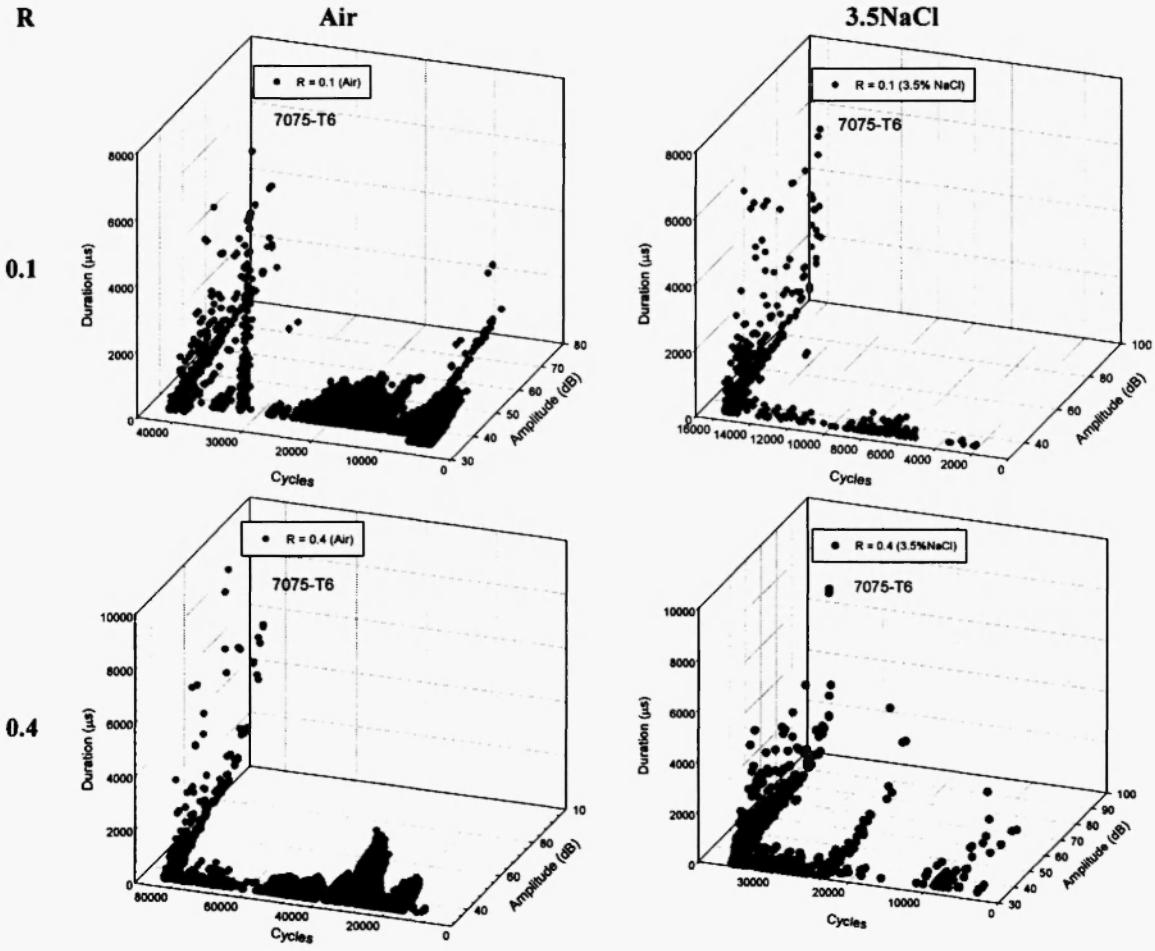

0.7

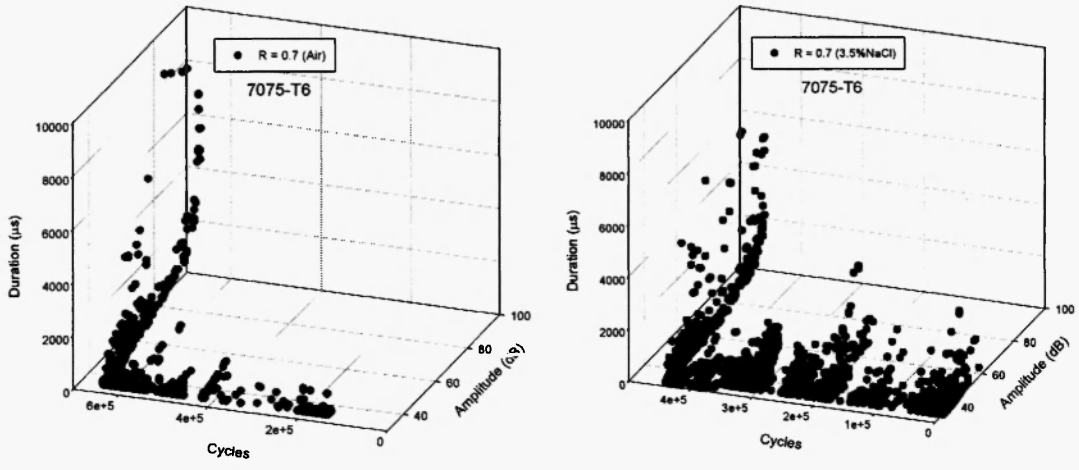

Fig. 6: A three dimensional view of the AE duration, amplitude and number of cycles corresponding to different stages.

Although the precise moment of crack initiation is difficult to define, however, stage I primarily included crack initiation and early growth up to 1.5 mm length from the notch tip. Accordingly, stage I exhibited the highest level of acoustic emission activity. For specimens tested at stress ratios of 0.1, 0.4 and 0.7 in air and in the presence of electrolyte Figs. 4 show plots of amplitude vs. duration whereas Figs. 6 classify the three stages in a three dimensional view of amplitude, duration and number of cycles for clarity. Crack nucleation shows an AE activity with amplitude and duration below 50dB and 200 s at stress ratio of 0.1, and decreases to 45dB and 100□s and 40dB and 20□s at stress ratios of 0.4 and 0.7, respectively. These AE characteristics can also be supported by the fact that at small R ratios (e.g. 0.1), the crack tip is subjected to larger strain rates that causes larger energy released in the form of stress waves (high amplitudes and large durations) leading to accelerated CGR's (see Figs. 2-3). On the contrary, at small R ratios the trend goes in the opposite way. A clear downward trend is observed in the amplitudes and duration as a function of increasing stress ratio that is attributed to micro-processes leading to lowering plastic deformation. As a general point of view, brittle fracture is characterized by high signal amplitude and shorter duration. However, ductile fracture is characterized by high plasticity at the crack tip which produces AE signals with apparently low amplitudes and longer durations /4, 11/. However, it was not possible to discriminate between the AE signals produced by the environmental factors (such as, hydrogen embrittlement and metal dissolution). Nevertheless, it is speculated that metal dissolution dominates lifetimes at higher stress ratios, while hydrogen embrittlement plays an increasing role at lower stress ratios (corresponding to shorter lives); this assertion is supported by changes in fracture surface morphology (from intergranular to transgranular, respectively) seen in Figs. 5.
The dislocation velocity is highly dependent upon the stress level, temperature and the presence of obstacles. AE signal due to dislocation movement is characterized by signal amplitudes of between ~20dB to ~45dB

/4,12/. Figs. 5 indicate a dominant cleavage fracture mode during stage I which is caused principally by the alignment/movement of a set of dislocations in the weak crystallographic direction and yielding a low AE amplitude (below ~ 50dB) at stress ratio of 0.7. At lower stress ratio (of 0.1), the main fracture mode was transgranular tearing which produced an increment in the amplitude of AE signals compared to the cleavage mode for specimens tested in air, as shown in Figs. 4 and 6. However, the fracture mode shifted from being transgranular in air to mainly intergranular fracture under corrosive electrolyte at all stress ratios. The corrosion processes also seemed to enhance the AE activity as can clearly be observed in Figs. 4 and 6 for specimens subjected to 3.5% NaCl electrolyte.

Based on fracture mechanics definition (thermodynamic balance), the energy released during the fracture process is directly related to the crack length, which decreases as the crack length increases /8,9/. Accordingly, experimental results revealed that stable crack propagation (stage II), presented a significant reduction of the AE activity (amplitude and duration); the effect was more severe in specimens tested in air, also seen in Figs. 4 and 6. The effect of stress ratio was surprisingly minimal during stage II. The final stage III which is generally characterized by unstable crack growth leading to catastrophic failure yielded substantially higher amplitudes and energy levels as indicated in Figs. 4 and 6 that were independent of the stress ratio. However, amplitudes of energy were somewhat higher for specimens subjected to corrosive environment.

CONCLUSIONS

Lifetime of AA7075-T6 was found to be sensitive to the presence of marine environment and lowering stress ratio. Acoustic emission aided in the understanding of crack initiation and growth mechanisms of the materials tested that may have otherwise been missed, however, requiring substantial preliminary testing, thresholds verification and parameter setup. Furthermore, the AE results confirmed that AE activity and its signal characteristics are highly dependent on material properties and specimen geometry. The application of AE was found to be robust in detecting failure events that could have otherwise been missed, however, the application of AE and data handling was cumbersome and time consuming. A clear shift in the microstructural features was observed when specimens were subjected to corrosive marine electrolyte or electrolytically charged with hydrogen.

ACKNOWLEDGMENTS

The research was carried out under ONR grant # N000140310540. The authors wish to acknowledge the support and guidance of ONR program manager Dr. Yapa Rajapakse. Thanks are also due to Dr. Vinod

Agarwala, senior scientist at ONR Global for his encouragement to undertake this task.

REFERENCES

1. Birnbaum, H., Mechanisms of hydrogen related fracture of metals, *Proceedings of Fourth International Conference on the Effects of Hydrogen on the Materials Behavior,* N.R. Moody and A.E. Thompson (Eds.), TMS publications, 639-660, 1989.
2. Gnyp, P., Phenomenological aspects of the influence of the cyclic loading parameters on corrosion-fatigue crack growth, *Soviet Materials Science*, 20(4), 344-348, 1984.
3. Gingell, A., King, J., The effect of frequency and microstructure on corrosion fatigue crack propagation in high strength aluminum alloys, *Acta Materialia*, **45**(9), 3855-3870, 1997.
4. *Non Destructive Testing Handbook*, American Society for Nondestructive Testing, Second Edition Vol. 5, 1987.
5. Yuyama, S., Kishi, T., Hisamatsu, Y., Fundamental aspects of ae monitoring on corrosion fatigue process in Austenitic stainless steel, *Journal of Materials for Energy systems*, **5**(4), 212-221, 1984.
6. Rongsheng, G. Modern acoustic emission technique and its application in aviation industry, *Ultrasonics*, **44**, 1025-1029, 2006.
7. Baxter, M., Pullin, R., Holford, K., Evans, S., Detection of fatigue crack growth in aircraft landing gear 4 point bend test specimens, *Engineering Materials*, **293-294**, 193-200, 2005.
8. Harris, D., Dunegan, H., Continuous monitoring of fatigue-crack growth by acoustic emission technique, *Experimental Mechanics*, 70-81, 1974
9. Wang, Z., Zhu, Z., Ke, W. Behavior of acoustic emission for low-strength structural steel during fatigue corrosion and corrosion fatigue, *Metallurgical Transactions A*, **22**A, 2677-2680, 1991.
10. Chaswal, V., Sasikala, G., Ray, S., Mannan, S., Raj, B., Fatigue crack mechanism in aged 9Cr-1Mo steel: Threshold and Paris regimes, *Materials Science and Engineering A*, **395**, 251-264, 2005.
11. Vallen, H., AE testing fundamentals, equipment, applications, *NDT.net*, 7:9, 2002.
12. Nam, K., Wei, R., Mal. A., Characteristics of acoustic emission waveforms generated by fatigue crack extension from corrosion sites in aluminum alloys, *Third FAA/DOE/NASA*, September 20-23, 1-8, 1999.
13. Shafiq, B., Agarwala, V. Corrosion and fatigue in high strength 7075-T6 aluminum: Life prediction issues, *AIAA - Journal of Aircraft*, **41**(2), 393-398, 2004.
14. Agarwala, V., What's eating us: Corrosion, *Naval Research Reviews*, **50**(4), 14-24, 1998.
15. Schijve, J., Cumulative damage analysis in aircraft structures and materials, *The Aeronautical Journal*, **74**, 517-532, 1970.
16. Saxena, A., Hudak, S., Review and extension of compliance information for common crack growth specimens, *International Journal of Fracture*, **14**(5), 453-468, 1978.

17. Beachem, C. A new model for hydrogen-assisted cracking (hydrogen embrittlement), *Metallurgical Transactions*, **3**, 437-451, 1972.
18. Turnbull, A. Modeling of environment assisted cracking, *Corrosion Science*, **34**(6), 921-960, 1993.
19. Tien, J., Thompson, A., Bernstein, I., Richards, R., Hydrogen transport by dislocations, *Metallurgical Transactions A*, **7A**, 821-829, 1976.
20. Quispitupa, A., Shafiq, B., Suárez, M., Uwakweh, O., Duque, N., Corrosion fatigue of high-strength aircraft structural alloys, *Journal of Aircraft*, **43**(3), 787-792, 2006